Article

Discovery Medicine 2025; 37(199): 1663–1676
https://doi.org/10.24976/Discov.Med.202537199.145

MDFI Promotes NSCLC Cell Proliferation and Migration by Modulating Autophagy

Guoliang Ma[1], Jing Lin[2], Miaolin Yu[3], Yuguo Ren[1,*]

[1]Department of Clinical Laboratory, Jinan City People's Hospital, Jinan People's Hospital Affiliated to Shandong First Medical University, 271100 Jinan, Shandong, China
[2]Hospital Infection Management Department, Qingdao Central Hospital, University of Health and Rehabilitation Sciences, 266042 Qingdao, Shandong, China
[3]Tumor Radiotherapy Department (II), Qingdao Central Hospital, University of Health and Rehabilitation Sciences, 266042 Qingdao, Shandong, China
*Correspondence: renyuguo_lw@163.com (Yuguo Ren)
Published: 20 August 2025

Background: Investigating the pathogenesis of non-small cell lung cancer (NSCLC) is crucial to identify early diagnostic markers and novel therapeutic targets. Myod family inhibitor (MDFI) has been associated with the occurrence and progression of tumors; however, its potential role in NSCLC remains uninvestigated. Therefore, this study explores the role of MDFI in NSCLC and its association with autophagy in disease progression.

Methods: *In vitro* cellular models and *in vivo* mouse models were used to assess the impact of MDFI in NSCLC progression. *MDFI* knockdown (sh-*MDFI*) and overexpression (oe-*MDFI*) cellular models were successfully established. Expression levels of *MDFI* were assessed using real-time quantitative polymerase chain reaction (RT-qPCR), while protein levels were analyzed using Western blot analysis. Cell proliferation, migration, and invasion abilities were determined using clonal formation, 5-ethynyl-2′-deoxyuridine (EdU), wound healing, and Transwell invasion assays, respectively. For rescue experiments, cells were subjected to 3-methyladenine (3-MA) treatment for 24 hours. The *in vivo* xenograft mouse model was established through subcutaneous injection of A549 cells. The expression levels of nuclear proliferation-associated antigen (Ki-67) were evaluated using immunohistochemistry (IHC).

Results: We observed significantly elevated MDFI expression in NSCLC cells ($p < 0.05$). *MDFI* overexpression promoted cell proliferation, migration, and invasion capabilities ($p < 0.05$); however, *MDFI* knockdown suppressed these cellular behaviors ($p < 0.05$). *MDFI* overexpression enhanced the microtubule-associated protein 1 light chain 3 II/I (LC3II/I) ratio and autophagy-related gene 12 (ATG12) expression, and decreased sequestosome-1 (p62) levels ($p < 0.05$), while *MDFI* knockdown showed an opposite trend ($p < 0.05$). Furthermore, 3-MA treatment counteracted *MDFI* overexpression-induced malignant behavior and autophagy of NSCLC cells ($p < 0.05$). The tumor experiment revealed that knocking down *MDFI* suppressed tumor growth and autophagy in nude mice ($p < 0.05$).

Conclusion: MDFI modulates NSCLC cell proliferation, migration, and invasion by regulating autophagy, underscoring MDFI as a potential biomarker and a novel therapeutic target.

Keywords: NSCLC; MDFI; autophagy; progression

Introduction

Non-small cell lung cancer (NSCLC) is the prevalent subtype of lung cancer (LC) [1]. The early onset of NSCLC is often insidious, with most patients exhibiting no typical clinical symptoms except occasional coughing and shortness of breath, resulting in delayed diagnosis and early curative management [2]. Currently, the treatment of NSCLC primarily involves a combination of surgical intervention, radiotherapy, and chemotherapy [3]. However, the therapeutic outcomes remain suboptimal in these patients, and their overall survival rate is poor [4]. Therefore, exploring the underlying mechanisms of NSCLC development is clinically crucial for identifying novel therapeutic targets and improving survival rates and prognosis. Although the specific mechanism of NSCLC development is yet to be fully explored, evidence suggests that the abnormalities in the autophagy system may contribute to its pathogenesis and metastasis [5].

Autophagy, a highly conserved biological process in eukaryotic cells, is activated under stress conditions such as hypoxia, starvation or extreme pH levels to decompose and recycle damaged or unnecessary cellular components; disruption of autophagy, whether through deficiency or overactivation, can result in diverse pathological conditions [6]. In cancer, autophagy plays a dual role, serving both as a tumor suppressor and a promoter [7]. Autophagy can inhibit tumor initiation and progression by degrading abnor-

mal cellular components or inducing a non-apoptotic pathway [8,9]. Additionally, it can also facilitate tumor cell proliferation, invasion, and metastasis [8,9]. In terms of tumor drug resistance, autophagy may support tumor-induced immune escape or enhance antitumor responses through interactions with components of the innate and acquired immune systems [10,11]. Growing evidence indicates that targeting autophagy could be a promising therapeutic option for NSCLC [12]. However, the relationship between autophagy and NSCLC is complex, and the function of autophagy is different in different tumor stages [5], highlighting the need to investigate its regulatory mechanism in NSCLC development. A comprehensive understanding of these underlying regulatory mechanisms could provide insights into novel clinical interventions.

Myod family inhibitor (MDFI) contains a highly conserved cysteine-rich domain [13]. Although MDFI plays a crucial role in embryonic development, bone and muscle formation, and tumor progression, its precise biological function is not fully understood [14,15]. MDFI is upregulated in many cancer types, including gastric, pancreatic, colorectal, breast, ovarian, and prostate cancers [16], and has been associated with the initiation and progression of gastric and colorectal cancers [17,18]. However, there is limited research on MDFI in NSCLC. Bioinformatics analysis has revealed that high MDFI expression is associated with poor prognosis in lung adenocarcinoma (LUAD) patients, indicating its potential as a prognostic marker [19]. However, the specific role and underlying mechanisms of MDFI in NSCLC pathogenesis remain incompletely understood.

To date, the role of MDFI and its relationship with autophagy in NSCLC have not been comprehensively explored. Therefore, this study investigates the role of MDFI and its association with autophagy in NSCLC progression, aiming to offer an experimental basis for potential clinical applications in managing NSCLC.

Materials and Methods

Cell Culture

Human bronchial epithelial cells (16HBE (YS003C)) were obtained from YaJi Biological (Shanghai, China), while human NSCLC lines A549 (CL-0016), H1299 (CL-0165), and HCC827 (CL-0094) were purchased from Pricella (Wuhan, China). These cell lines were cultured in Roswell Park Memorial Institute 1640 (RPMI 1640) medium containing 10% fetal bovine serum (FBS; PM150110B, Procell, Wuhan, China) and 1% penicillin-streptomycin (CSH9024, Chemstan, Wuhan, China). All cell lines were authenticated using short tandem repeat profiling and examined for contamination employing mycoplasma testing.

Short hairpin RNA targeting *MDFI* (sh-*MDFI*) and a negative control (sh-NC) lentiviral particles, along with *MDFI* overexpression plasmid (oe-*MDFI*) and corresponding control (oe-NC), were obtained from GenePharma (Shanghai, China). Lentiviral constructs (pLVX) for sh-NC and sh-*MDFI* were obtained from Sangon (Shanghai, China). Lentiviruses were transfected into cells following the manufacturer's protocols. Stable knockdown cells were selected employing puromycin (P8230, Solarbio, Beijing, China). Transfection of oe-*MDFI* and oe-NC plasmids was performed using Lipofectamine 2000 (11668019, Thermo Fisher Scientific, Waltham, MA, USA), and transfection efficiency was evaluated 48 hours after transfection.

Additionally, for rescue experiments, cells were treated with 5 mM 3-methyladenine (3-MA, MCE, HY-19312, Shanghai, China) for 24 hours. Cells were divided into the following groups: control (untreated A549 or HCC827 cell lines), sh-NC, oe-NC, sh-*MDFI*, oe-*MDFI*, oe-*MDFI*+dimethyl sulfoxide (DMSO, 67-68-5, Sinopharm, Shanghai, China), and oe-*MDFI*+3-MA. The nucleotide sequences of oe-NC and oe-*MDFI* were given in the **Supplementary file**, while the targeting sequences of sh-NC and sh-*MDFI* were as follows:

sh-*MDFI*: Sense: 5′-GCAAGAAGAGTAAGAGCAGCA-3′, Antisense: 5′-TGCTGCTCTTACTCTTCTTGC-3′; sh-NC: Sense: 5′-ACATCGGCAGGGAAAAGAGAA-3′, Antisense: 5′-TTCTCTTTTCCCTGCCGATGT-3′.

Real-time Quantitative Polymerase Chain Reaction (RT-qPCR)

The RT-qPCR assay was performed using a previously described protocol [20]. Total RNA was extracted using TRIzol reagent (15596-018, Invitrogen, Carlsbad, CA, USA). Purity and concentration of RNA were determined by measuring absorbance at A260 nm and A280 nm employing a spectrophotometer (Nanodrop 2000, Thermo Fisher Scientific, Waltham, MA, USA). Total RNA was converted into cDNA using a reverse transcription kit (18064-014, Invitrogen, Carlsbad, CA, USA). RT-qPCR was performed using the cDNA as the template with a SYBR-Green PCR kit (SR4110, Solarbio, Beijing, China) on a PCR system (ABI 7500, Foster, CA, USA). Relative expression levels of target genes were calculated using the $2^{-\Delta\Delta Ct}$ method, with glyceraldehyde-3-phosphate dehydrogenase (*GAPDH*) serving as an internal reference. The primers used in RT-qPCR were as follows:

MDFI:
Forward: 5′-CCACCGGAAGTTGCAGACA-3′;
Reverse: 5′-GGAACTCGCAGAACAGGCA-3′;
GAPDH:
Forward: 5′-GAGCCACATCGCTCAGACACC-3′;
Reverse: 5′-TGACAAGCTTCCCGTTCTCAGC-3′.

Western Blotting

Western blotting was conducted following a previously described protocol [21]. Total proteins were extracted

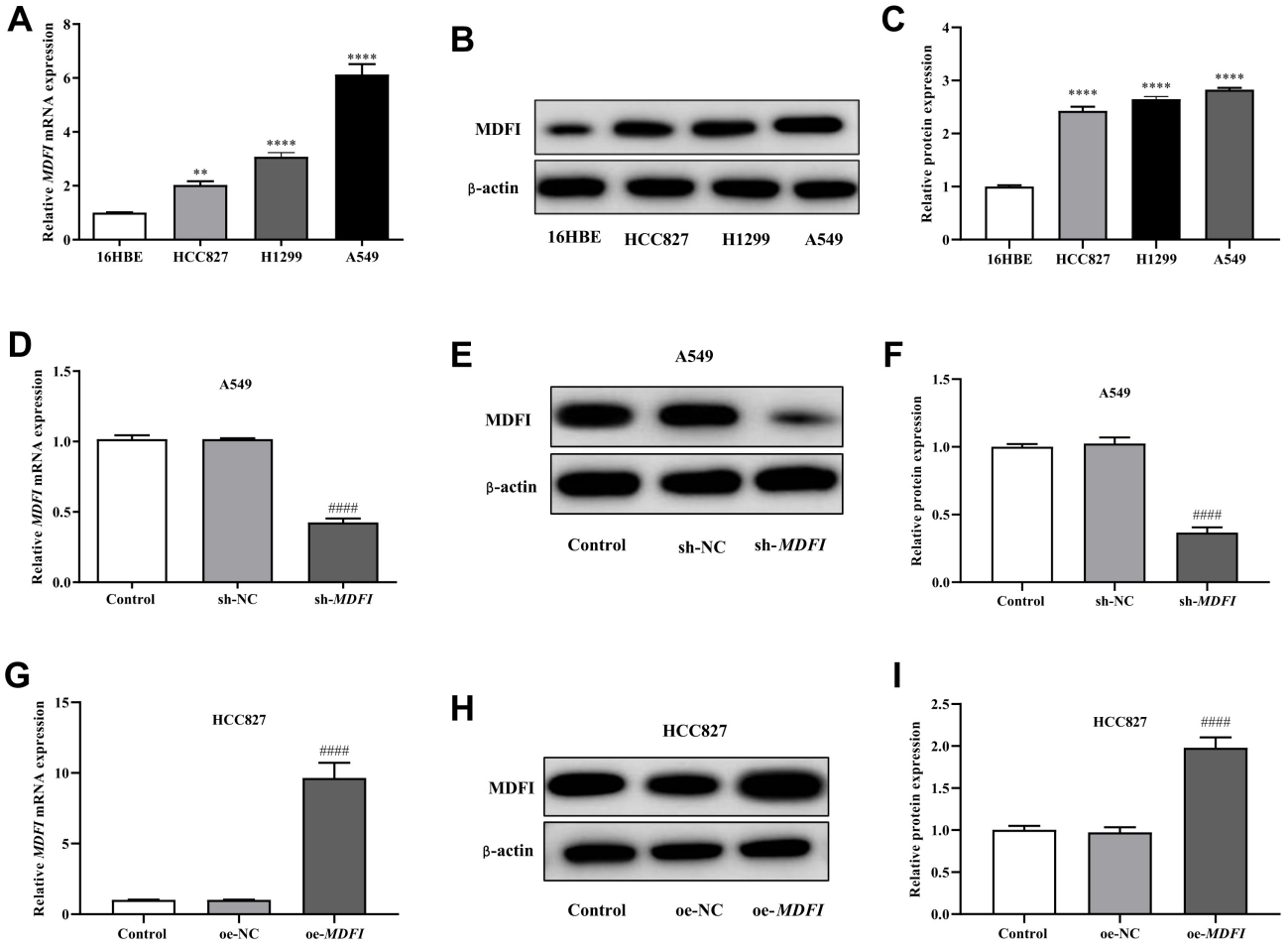

Fig. 1. Expression of MDFI in NSCLC cells. (A–C) Elevated MDFI expression in NSCLC cell lines (n = 3). (D–I) MDFI expression levels in NSCLC cells after MDFI knockdown or overexpression (n = 3). $^{**}p < 0.01$, $^{****}p < 0.0001$, compared to the 16HBE group. $^{\#\#\#\#}p < 0.0001$, compared to the sh-NC or oe-NC group. NSCLC, non-small cell lung cancer; MDFI, Myod family inhibitor; sh, short hairpin; NC, negative control; oe, overexpression. The control group represents the untreated A549 or HCC827 cell lines.

using radio-immunoprecipitation assay lysate (P0013B, Beyotime, Shanghai, China) and subsequently quantified by employing the bicinchoninic acid kit (P0010S, Beyotime, Shanghai, China). Equal amounts of proteins (30 µg) were separated by sodium dodecyl sulfate-polyacrylamide gel electrophoresis and transferred onto polyvinylidene fluoride (PVDF) membranes (IPVH00010, Millipore, Boston, MA, USA). The membrane was blocked with 5% skim milk and incubated overnight at 4 °C with the following primary antibodies: anti-MDFI (1:1000, A13709, ABclonal, Wuhan, China), anti-autophagy-related gene 12 (ATG12) (1:1000, 2010, CST, Danvers, MA, USA), anti-microtubule-associated protein 1 light chain 3 (LC3) (1:1000, 2775, CST, Danvers, MA, USA), anti-sequestosome-1 (p62) (1:1000, 8025, CST, Danvers, MA, USA), and anti-β-actin (1:1000, 4967, CST, Danvers, MA, USA). The next day, the membranes were incubated with horseradish peroxidase (HRP)-conjugated secondary antibody (1:2000, 7074, CST, Danvers, MA, USA) for 1 hour at room temperature. Protein bands were developed using enhanced chemiluminescence reagent (P0018M, Beyotime, Shanghai, China) and observed under a luminescent image analyzer (5200, Tanon, Shanghai, China). Gray values of these bands were quantified using Image J software (version 1.8, NIH, Rockville, MD, USA).

5-Ethynyl-2′-deoxyuridine (EdU) Assay

EdU assay was performed using a previously described method [22]. Cells were seeded in 24-well plates at a density of 5×10^4 cells/well and incubated for 24 hours. EdU working solution (C0075S, Beyotime, Shanghai, China) was mixed with a complete medium and added to each group. Following incubation, cells were fixed with 4% paraformaldehyde (P0099, Beyotime, Shanghai, China) for 15 minutes. After this, a permeabilization buffer (P0097, Beyotime, Shanghai, China) was added and incubated again for 15 minutes. Then the cells were incubated with the Apollo reaction solution in the dark for 30 minutes, followed by staining with 4′,6-diamidino-2-phenylindole (DAPI, C0065, Solarbio, Beijing, China) for

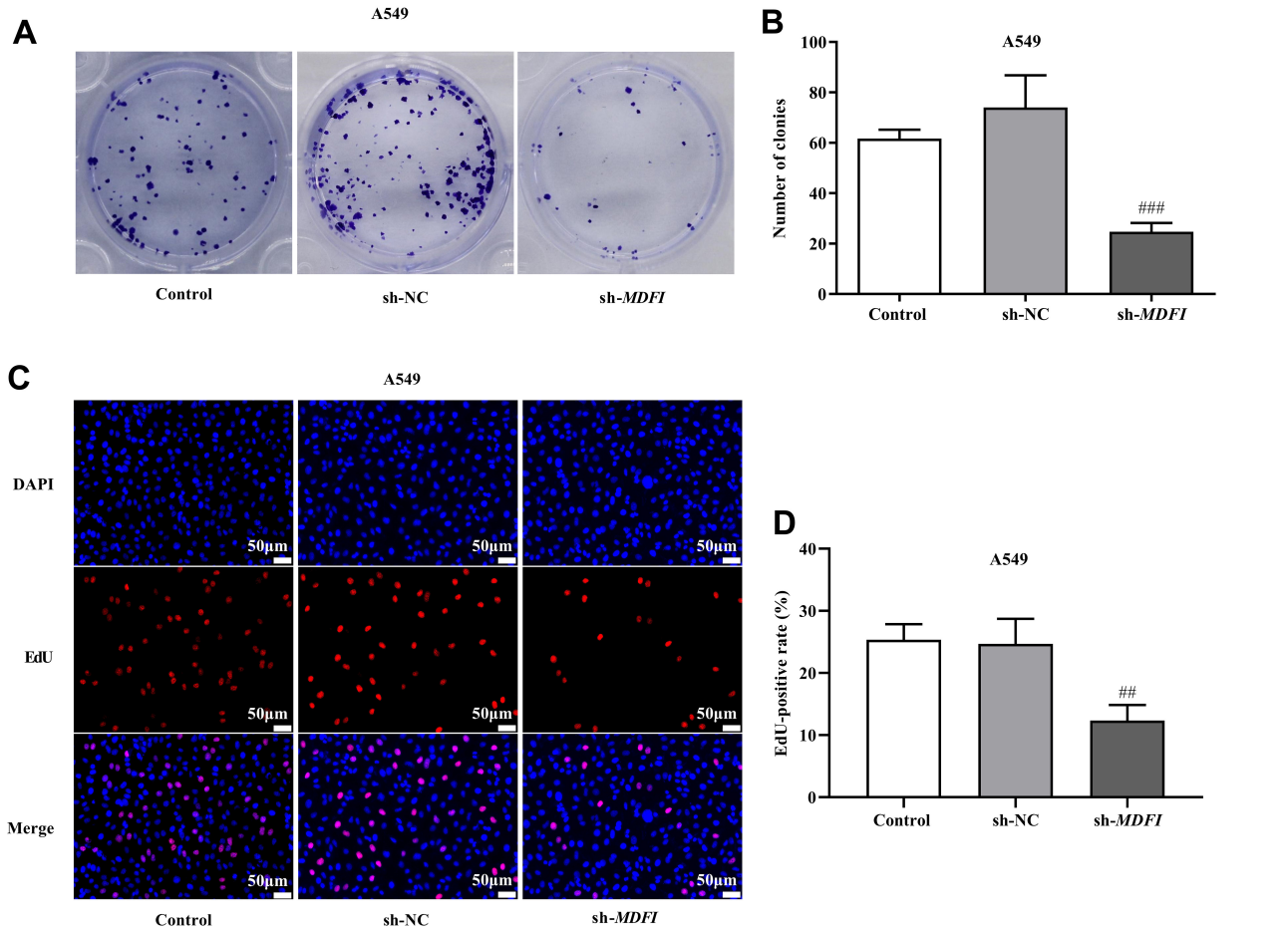

Fig. 2. Impact of *MDFI* knockdown on A549 cell proliferation. (A,B) Effect of *MDFI* knockdown on cell colony forming ability (n = 3). (C,D) Effect of *MDFI* knockdown on cell proliferation detected through EdU method (scale bar: 50 μm, magnification: 200×) (n = 3). $^{\#\#}p < 0.01$, $^{\#\#\#}p < 0.001$, compared to the sh-NC group. DAPI, 4′,6-diamidino-2-phenylindole; EdU, 5-Ethynyl-2′-deoxyuridine.

10 minutes. Stained cells, the DAPI state (blue) and fluorescent EdU (red), were observed using a fluorescence microscope (FSX100, Olympus, Tokyo, Japan) in the dark. Finally, EdU-positive cells were quantified, and the proliferation rate was determined as follows: EdU-positive cells (%) = (Number of EdU cells/total number of DAPI-stained cells) × 100%.

Colony Formation Assay

Colony formation assay followed a previously published method [23]. Cells were seeded in 6-well plates at a density of 1×10^3 cells/well and incubated for 14 days. After that, cells were fixed with 4% paraformaldehyde and stained with crystal violet solution (C8470, Solarbio, Beijing, China). Stained cell colonies were photographed using a digital camera (CKX53, Olympus, Tokyo, Japan).

Wound Healing Assay

As previously described [24], cells were inoculated into 6-well plates and allowed to reach confluence. Vertical scratches were created in the cell monolayer using a sterilized 100 μL pipette tip, and the detached cells were gently washed away. After 24 hours of incubation under standard culture conditions, the migration distance of the scratches (wound) was examined using Image J software (version 1.8, NIH, Rockville, MD, USA) to evaluate cell migration capability. The wound healing rate was determined as follows: Healing rate (%) = (Width $_{0\,h}$ – Width $_{24\,h}$)/Width $_{0\,h}$ × 100%.

Transwell Assay

The Transwell assay followed a previously described protocol [25]. A 60 μL of matrix glue (Matrigel), diluted in serum-free medium at a ratio of 1:4, was added to the upper layer of the Transwell chamber (3413, Corning, Corning, NY, USA) and allowed to coagulate. Subsequently, 200 μL of cell suspension (1×10^5 cells/mL) was added to the upper layer, while 700 μL of complete medium was added to the lower compartment as a chemoattractant. After 48 hours of incubation, the cells were fixed with 4% paraformaldehyde and stained with crystal violet. The number of cells

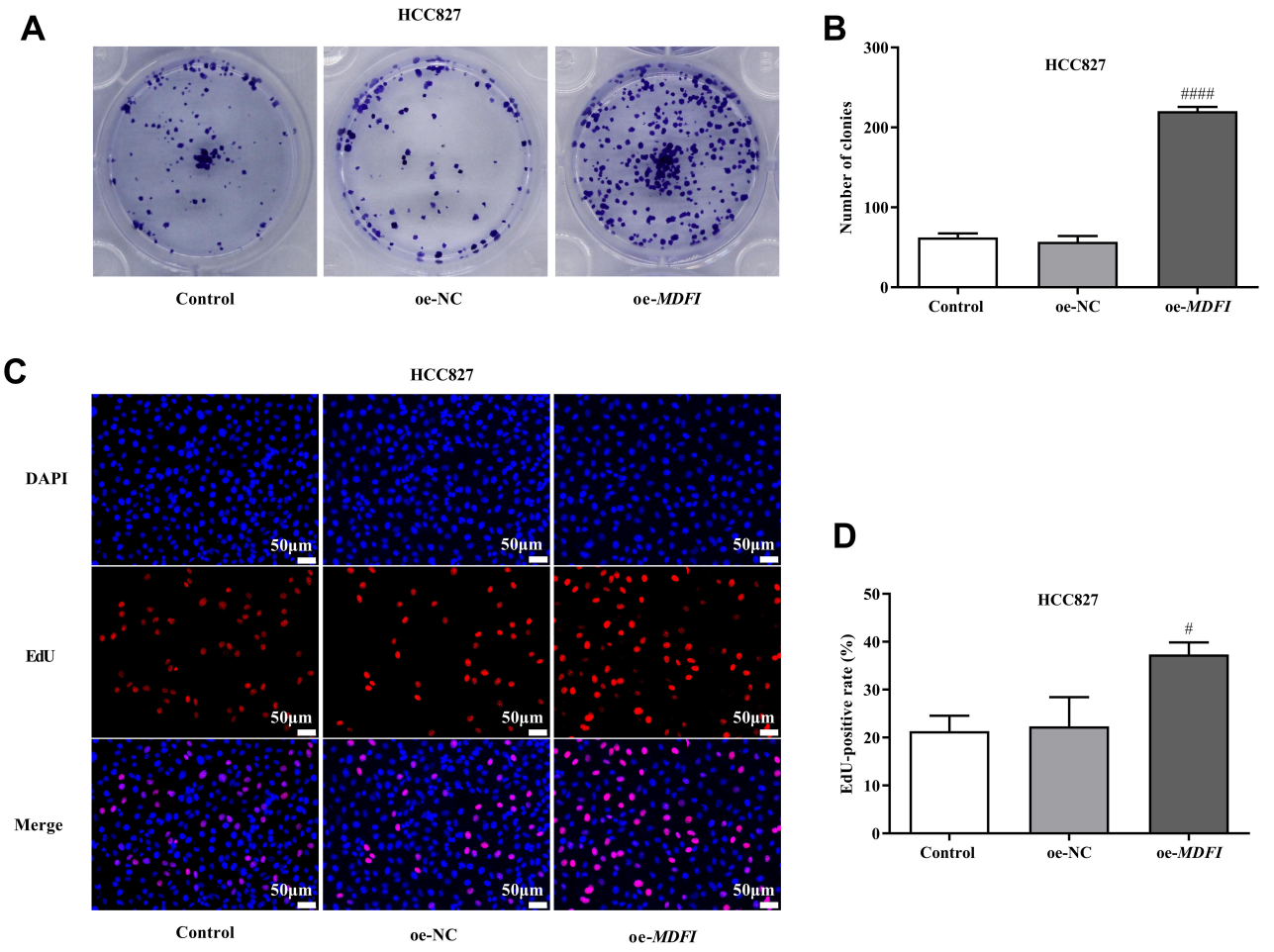

Fig. 3. Impact of *MDFI* overexpression on HCC827 cell proliferation. (A,B) Effect of *MDFI* overexpression on cell colony forming ability (n = 3). (C,D) The effect of *MDFI* overexpression on cell proliferation was detected by the EdU method (scale bar: 50 μm, magnification: 200×) (n = 3). $^{\#}p < 0.05$, $^{\#\#\#\#}p < 0.0001$, compared to the oe-NC group.

that migrated across the membrane was observed under a microscope (BX53, Olympus, Japan) and quantified using Image J software (version 1.8, NIH, Rockville, MD, USA).

Establishing a Xenograft Model

The Xenograft model was established using a previously described protocol [26]. Nine female BALB/c nude mice (4 to 5 weeks old and weighing 18–20 g) were purchased from Beijing Vital River Laboratories (SCXK (Jing) 2021-0011). Mice were housed in a semi-barrier environment under constant temperature and humidity, with access to sterilized food and water. Mice were randomly divided into 3 groups (n = 3): control (A549 cells), sh-NC (A549 cells transfected with negative control shRNA), and sh-*MDFI* (A549 cells transfected with *MDFI*-targeting shRNA).

Each mouse was administered with 2×10^6 cells injected into the right axillary region. They were monitored daily for activity, food, water intake, and symptoms of tumor development. A localized wheal was observed at the site of injection shortly after inoculation. One week after the injection, visible subcutaneous nodules were found in all mice. By day ten, palpable masses with irregular shapes and well-defined boundaries (diameter) protruded from the skin, indicating successful establishment of the NSCLC xenograft model.

Mice were euthanized by cervical dislocation at week four, and tumors were carefully excised. Tumors were weighed, photographed, and their volumes were calculated as follows:

$V = (L \times W^2)/2$, where V is tumor volume, L is tumor length, and W is tumor width.

Immunohistochemistry (IHC)

Tumor tissues obtained from mice were fixed, dehydrated, embedded in paraffin, and sectioned 5 μm-thick slices, which were stored at room temperature or 4 °C. After baking, dewaxing, hydration, and antigen repair via microwave heating, the sections were incubated in a 0.3% H_2O_2 solution (H48022, IPODIX, Wuhan, China)

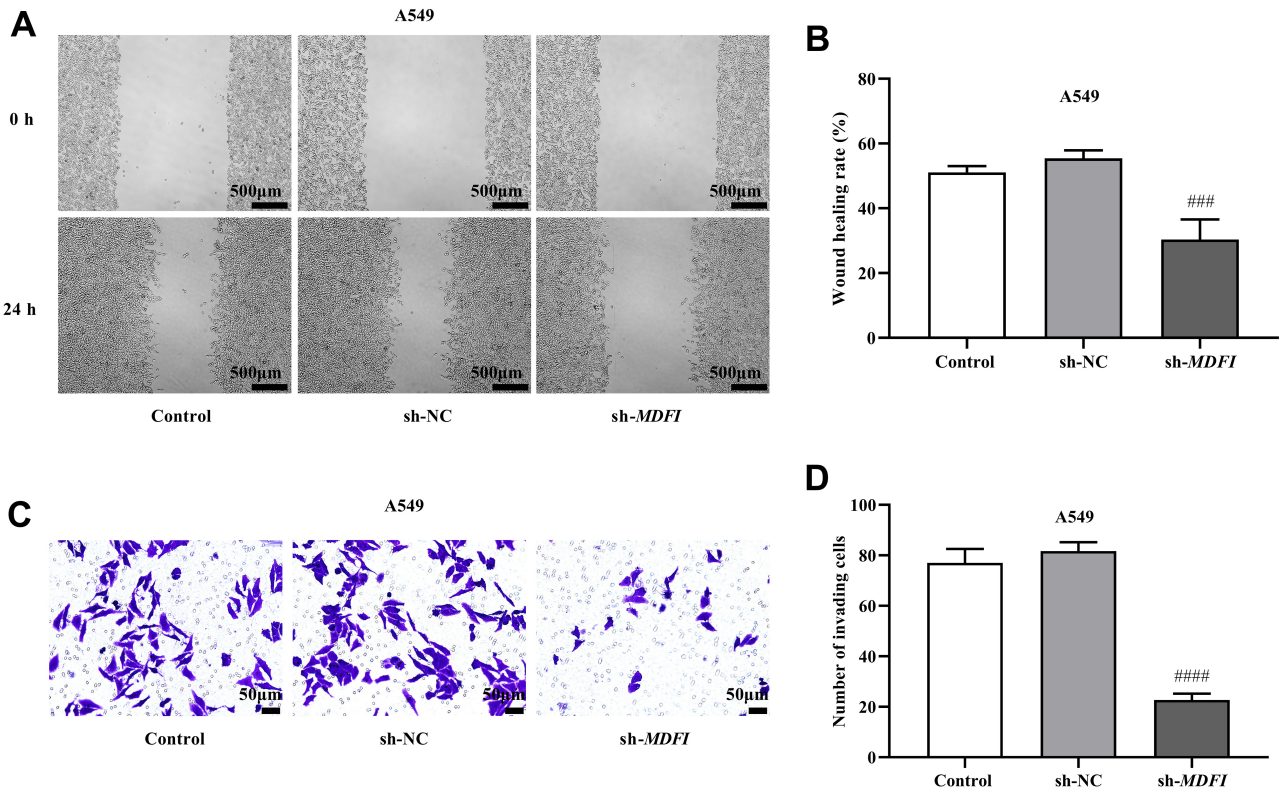

Fig. 4. Impact of *MDFI* silencing on A549 cell migration and invasion. (A,B) Cell migratory ability was detected using a wound healing assay (scale bar: 500 μm, magnification: 40×) (n = 3). (C,D) The invasion ability was assessed using the Transwell assay (scale bar: 50 μm, magnification: 200×) (n = 3). $^{###}p < 0.001$, $^{####}p < 0.0001$, compared to the sh-NC group.

for 25 minutes in the dark at room temperature to block endogenous peroxidase. After that, these sections were blocked with 30% goat serum (C0265, Beyotime, Shanghai, China) and incubated overnight at 4 °C with anti-Ki-67 antibody (Ki-67, nuclear proliferation-associated antigen; 1:500, A20018, ABclonal, Wuhan, China). After washing, tissue sections were incubated with an appropriate secondary antibody (RK50015, ABclonal, Wuhan, China). Then the sections were stained using DAB chromogenic solution (DA1010, Solarbio, Beijing, China), followed by counterstaining with hematoxylin (C0107, Beyotime, Shanghai, China). After that, the tissue sections were sequentially dehydrated in a gradient of ethanol and cleared in xylene. Once air-dried, the tissue section was mounted using neutral resin. Expression of Ki-67 was observed under a light microscope (BX51T-72F, Olympus, Japan), and staining results were evaluated using a double-scoring method. The presence of brownish-yellow nuclear granules was considered indicative of positive staining. A sample with more than 10% of nuclear positivity was considered to exhibit positive Ki-67 expression.

Statistical Analysis

Statistical analysis was conducted using GraphPad Prism software (version 8.0, GraphPad Software, San Diego, CA, USA). Data were expressed as mean ± standard deviation. One-way analysis of variance followed by Tukey's post hoc test was used for comparisons among multiple groups, while an unpaired *t*-test was applied for comparison between two groups. All experiments were performed in triplicate (n = 3), and a *p*-value of <0.05 was considered statistically significant.

Results

Expression of MDFI in Human NSCLC Cells

MDFI mRNA expression was significantly elevated in NSCLC cell lines compared to 16HBE cells (Fig. 1A) ($p < 0.05$), and a similar trend was observed at the protein level (Fig. 1B,C, $p < 0.05$). Overall, MDFI expression levels in NSCLC cells differed significantly from those in normal 16HBE (Fig. 1A–C, $p < 0.05$). Among NSCLC cell lines, MDFI expression was highest in A549 and lowest in HCC827 (Fig. 1A–C, $p < 0.05$). Based on these results, A549 and HCC827 cells were selected for subsequent functional assays.

To investigate the role of MDFI in NSCLC progression, a series of cell function experiments were conducted by overexpressing the *MDFI* gene in HCC827 cells and knocking down the *MDFI* gene in A549 cells. Transfec-

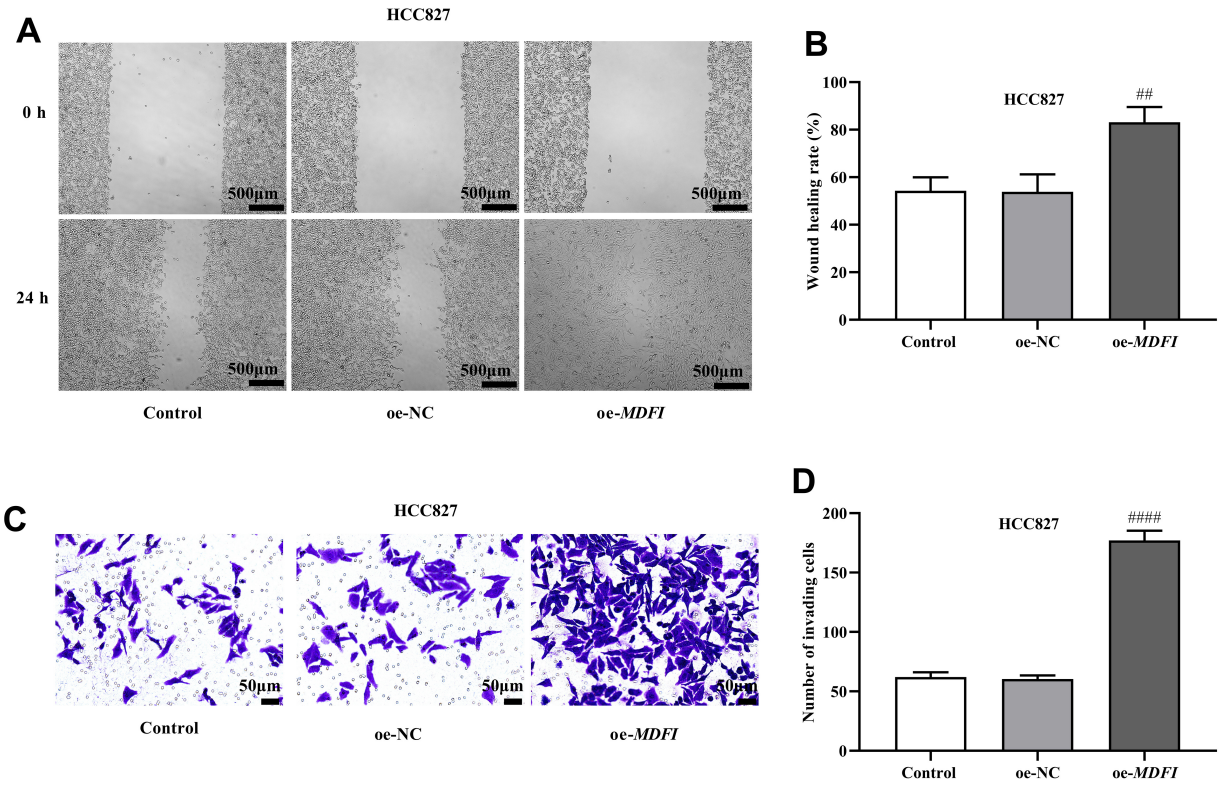

Fig. 5. Impact of *MDFI* overexpression on HCC827 cell migration and invasion. (A,B) Cell migratory ability was detected using a wound healing assay (scale bar: 500 μm, magnification: 40×) (n = 3). (C,D) The invasion ability was determined using the Transwell assay (scale bar: 50 μm, magnification: 200×) (n = 3). $^{\#\#}p < 0.01$, $^{\#\#\#\#}p < 0.0001$, compared to the oe-NC group.

tion with sh-*MDFI* effectively reduced MDFI expression in A549 cells (Fig. 1D–F, $p < 0.05$), while transfection with oe-*MDFI* substantially elevated its level in HCC827 cells (Fig. 1G–I, $p < 0.05$). These findings indicate the successful modulation of MDFI expression levels in these cell lines.

MDFI Expression Modulates NSCLC Cell Proliferation

MDFI knockdown significantly decreased the number of cell clones, while *MDFI* overexpression led to an increase in colony formation (Fig. 2A,B, Fig. 3A,B, $p < 0.05$). Similarly, the percentage of EdU-positive cells reduced after *MDFI* knockdown and increased with *MDFI* overexpression (Fig. 2C,D, Fig. 3C,D, $p < 0.05$). These results indicate that MDFI upregulation promotes NSCLC cell proliferation.

MDFI Overexpression Promotes NSCLC Cell Migration and Invasion

The impact of MDFI on NSCLC cell migration and invasion was further assessed. *MDFI* knockdown substantially inhibited the migratory capability of NSCLC cells, whereas its overexpression increased cell migration (Fig. 4A,B, Fig. 5A,B, $p < 0.05$). Similarly, *MDFI* knockdown suppressed the invasion ability of NSCLC cells, while its overexpression led to increased invasion (Fig. 4C,D, Fig. 5C,D, $p < 0.05$).

MDFI Regulates Autophagy in NSCLC Cells

Interestingly, analysis using the HitPredict database (https://www.hitpredict.org/interaction.php?Value=296750) indicated a potential interaction between MDFI and ATG12. To investigate whether MDFI impacts autophagy in NSCLC cells, the expression levels of crucial autophagy-related proteins were assessed in cells with altered MDFI expression. Findings revealed that *MDFI* knockdown led to a decrease in the microtubule-associated protein 1 light chain 3II/I (LC3II/I) ratio and ATG12 expression, along with an increase in the p62 level (Fig. 6A–D, $p < 0.05$). In contrast, *MDFI* overexpression resulted in an increased LC3II/I ratio and ATG12 expression, accompanied by a decreased p62 level (Fig. 6E–H, $p < 0.05$). These results indicate that MDFI may promote autophagy in NSCLC cells.

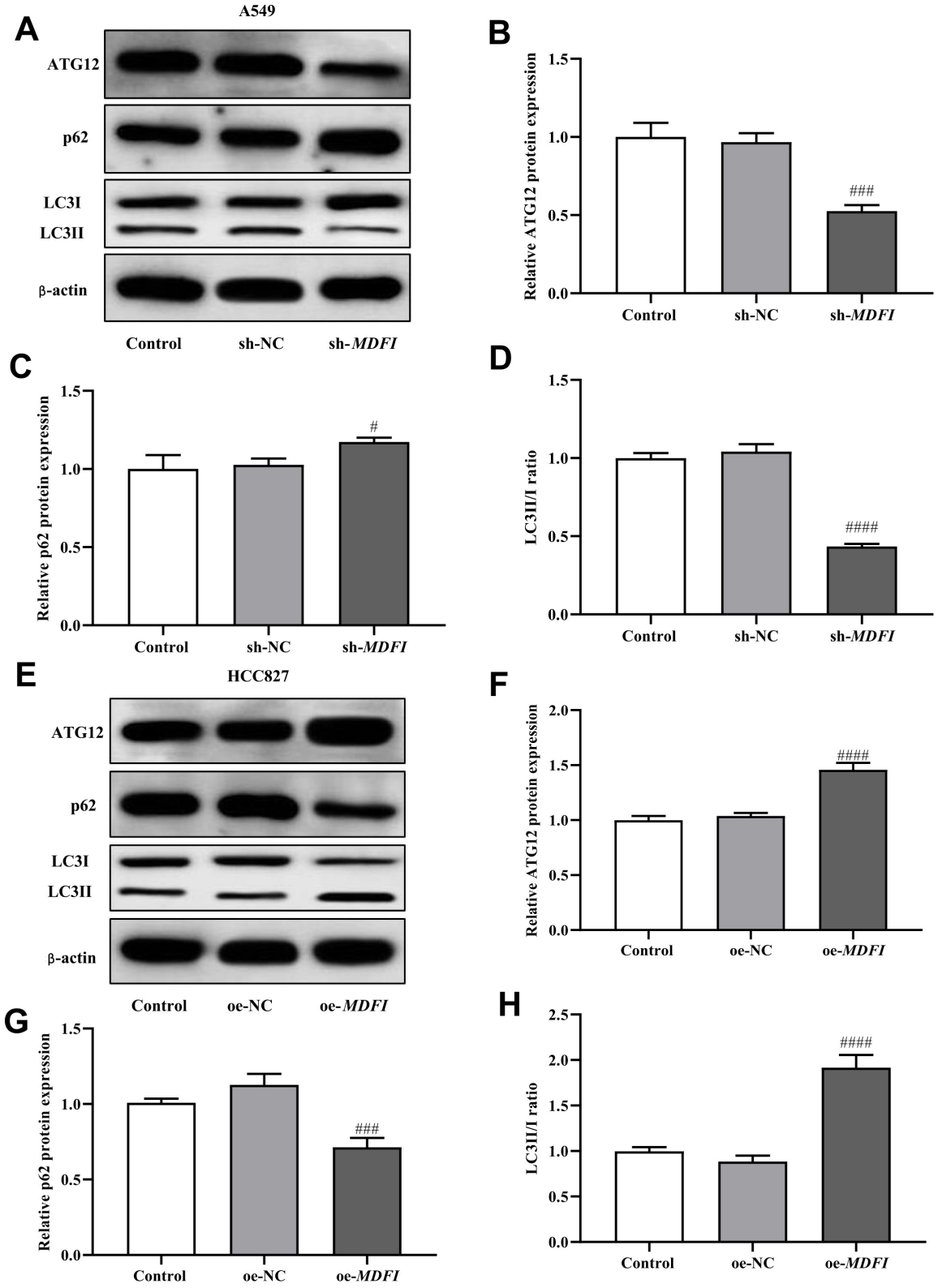

Fig. 6. Impact of MDFI expression levels on autophagy in NSCLC cells. (A–D) ATG12, p62, and LC3II/I expression and statistical graph in NSCLC cells with MDFI knockdown (Western blot analysis; n = 3). (E–H) ATG12, p62, and LC3II/I expression and statistical graph in NSCLC cells with MDFI overexpression (Western blot analysis; n = 3). $^{\#}p < 0.05$, $^{\#\#\#}p < 0.001$, $^{\#\#\#\#}p < 0.0001$, compared to the sh-NC or oe-NC group. ATG12, autophagy-related gene 12; LC3II/I, microtubule-associated protein 1 light chain 3II/I; p62, sequestosome-1.

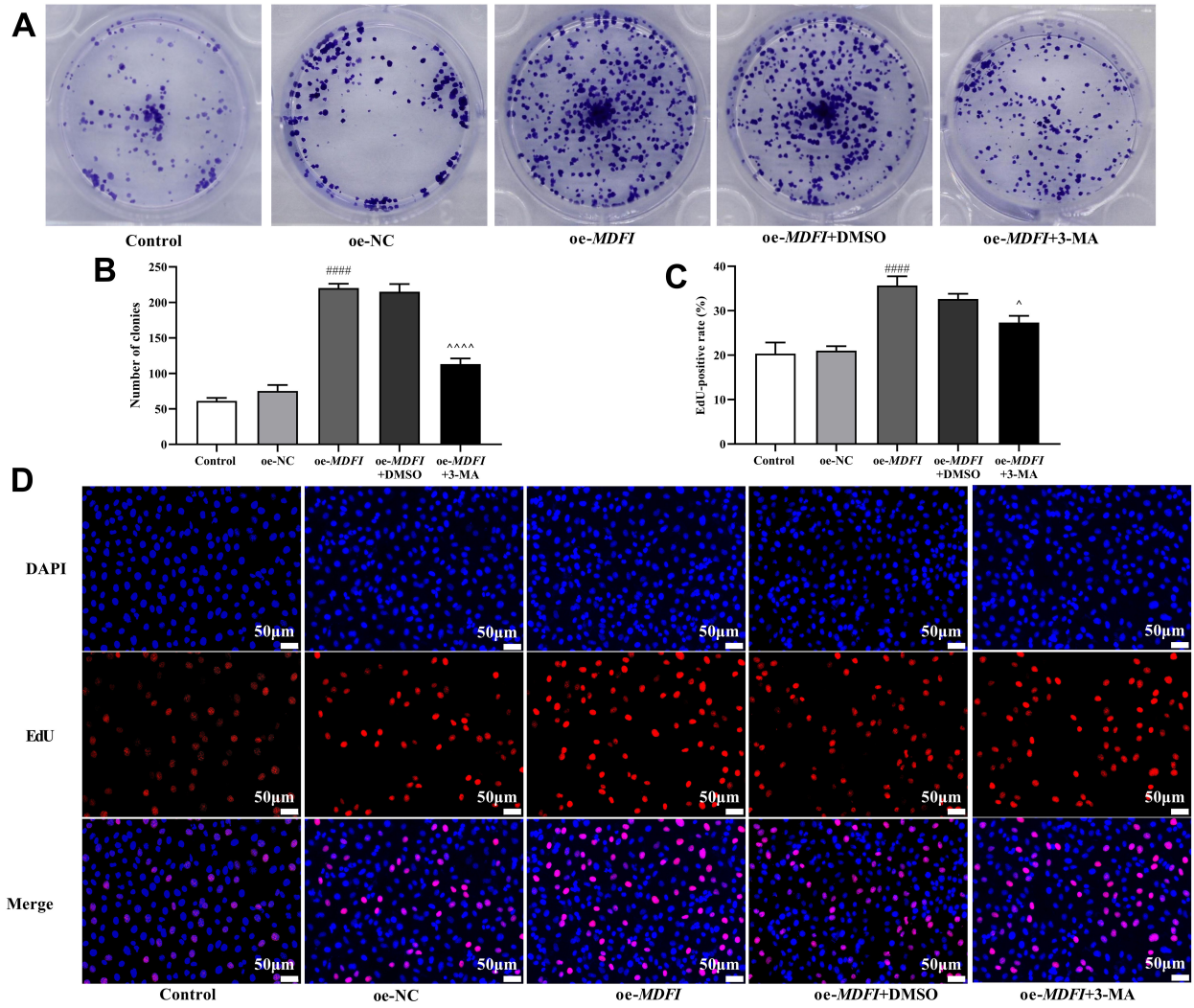

Fig. 7. Impact of 3-MA treatment on the proliferation of *MDFI*-overexpressing HCC827 cells. (A,B) 3-MA treatment inhibited the increase in colony formation induced by *MDFI* overexpression (n = 3). (C,D) 3-MA treatment suppressed the increase in EdU-positive rate induced by *MDFI* overexpression (scale bar: 50 μm, magnification: 200×) (n = 3). $^{\#\#\#\#}p < 0.0001$, compared to the oe-NC group. $^{\wedge}p < 0.05$, $^{\wedge\wedge\wedge\wedge}p < 0.0001$, compared to the oe-MDFI+DMSO group. 3-MA, 3-methyladenine; DMSO, dimethylsulfoxide.

MDFI Promotes the Malignant Behavior of NSCLC Cells by Regulating Autophagy

To examine whether MDFI promotes the malignant behavior of NSCLC cells through autophagy, rescue experiments were performed using 3-MA, an autophagy inhibitor. Treatment with 3-MA substantially decreased the proliferation, wound healing capacity, and invasion ability induced by *MDFI* overexpression in NSCLC cells (Figs. 7,8, $p < 0.05$). Moreover, MDFI-induced increase in the LC3II/I ratio and ATG12 expression, along with a decrease in p62 levels, was reversed by 3-MA treatment (Fig. 9, $p < 0.05$). These observations suggest that the pro-malignant behavior of *MDFI* overexpression in NSCLC cells is mediated through autophagy.

MDFI Knockdown Inhibits the Malignant Progression of NSCLC In Vivo

Based on the findings of cellular experiments, we assume that *MDFI* knockdown inhibits the progression of NSCLC by inhibiting autophagy and malignant cellular behaviors. To ensure experimental rigor and validate these results *in vivo*, tumor xenograft assays were performed in nude mice. *MDFI* knockdown (sh-*MDFI*) significantly decreased tumor growth, as evidenced by reduced tumor volume and weight (Fig. 10A–C, $p < 0.05$). Furthermore, the Ki-67 positivity rate was substantially reduced in the sh-*MDFI* group compared to the sh-NC group (Fig. 10D,E, $p < 0.05$). Consistent with *in vitro* findings, *MDFI* knockdown resulted in a decreased LC3II/I ratio and ATG12 expression along with increased p62 level in mouse tumor tissue (Fig. 10F–I, $p < 0.05$).

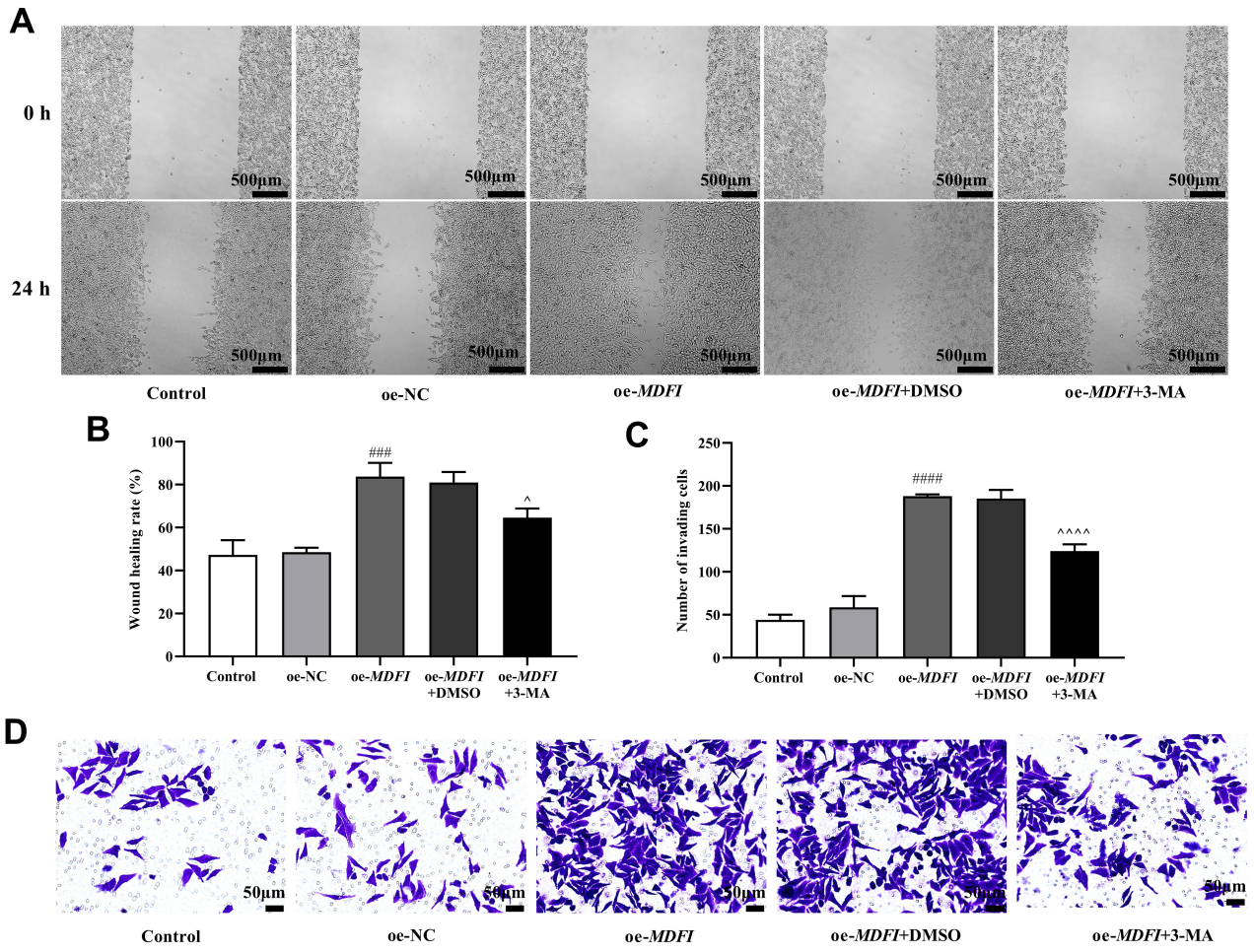

Fig. 8. Impact of 3-MA treatment on the migration and invasion of *MDFI*-overexpressing HCC827 cells. (A–D) 3-MA treatment suppressed an increase in cell migration (scale bar: 500 μm, magnification: 40×) and invasion (scale bar: 50 μm, magnification: 200×) induced by *MDFI* overexpression (n = 3). $^{###}p < 0.001$, $^{####}p < 0.0001$, compared to the oe-NC group. $^{\wedge}p < 0.05$, $^{\wedge\wedge\wedge\wedge}p < 0.0001$, compared to the oe-MDFI+DMSO group.

Discussion

NSCLC is a general term for all malignant tumors originating from the bronchial mucosa epithelium or lung glands, excluding small-cell lung cancer [27]. The known risk factors for NSCLC include smoking, exposure to cooking oil fumes, environmental pollution, a family history of LC, chronic lung diseases, and occupational exposure to carcinogens [28]. Although advances in health sciences have improved the prevention, clinical diagnosis, and treatment of NSCLC, the underlying molecular mechanisms of the disease remain unclear, and current treatment approaches still have significant limitations. Most NSCLC patients experience a high recurrence rate and metastasis after conventional treatment [29]. Hence, exploring the molecular mechanisms underlying NSCLC progression is crucial for enhancing diagnostic and treatment strategies.

MDFI plays a crucial role across various tissues and species; however, there are limited studies on its involvement in cancer [30]. While initially considered a tumor suppressor in tumorigenesis [31], growing evidence indicates that MDFI may show oncogenic properties in certain cancer types. Increased MDFI expression has been reported in colorectal cancer (CRC) and gastric cancer (GC) tissues [16–18]. In GC, elevated MDFI expression levels are associated with poor prognosis, and *MDFI* knockdown has been observed to inhibit Helicobacter pylori-induced cell proliferation and glycolysis [18]. Similarly, in CRC, MDFI stimulates HCT116 cell growth [16] and promotes cell proliferation and chemoresistance by interacting with integrin subunit beta 4 (ITGB4)/laminin subunit beta 3 (LAMB3) to activate the AKT signaling pathway [17]. These investigations indicate that MDFI may function as a tumor promoter in GC and CRC.

Furthermore, MDFI has been highly expressed in LUAD and is presumed to be associated with tumor proliferation and metastasis [19]. However, the functional role and underlying mechanism of MDFI in NSCLC pro-

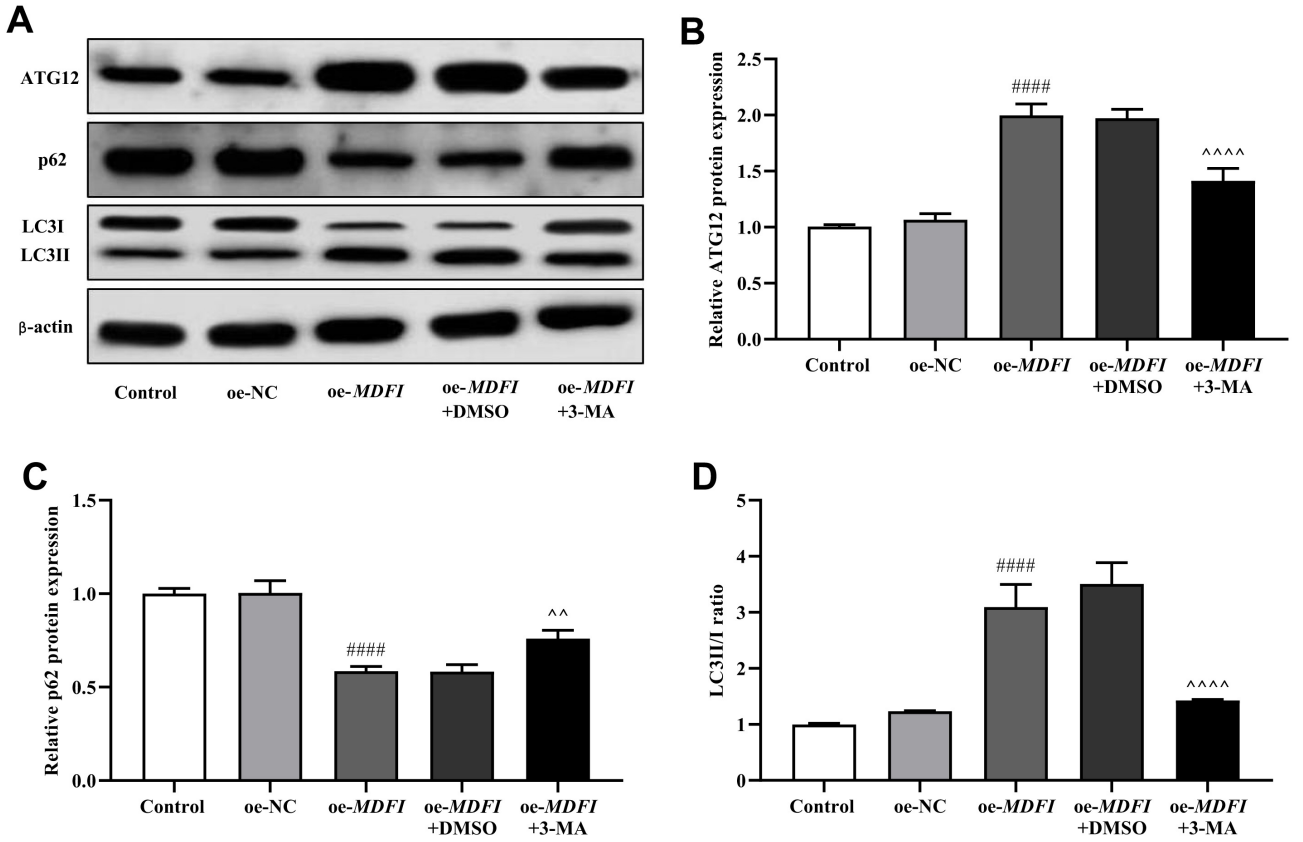

Fig. 9. 3-MA counteracted the impact of *MDFI* overexpression on the autophagy-related protein expression in HCC827 cells. (A) Western blot analysis of ATG12, p62, and LC3II/I expression levels (n = 3). (B–D) Graphical presentation of ATG12 and p62 expression, and LC3II/I ratio (n = 3). $^{\#\#\#\#}p < 0.0001$, compared to the oe-NC group. $^{\wedge\wedge}p < 0.01$, $^{\wedge\wedge\wedge\wedge}p < 0.0001$, compared to the oe-MDFI+DMSO group.

gression remain largely unexplored. In our study, we observed a significant increase in the expression of MDFI in NSCLC cells. To further uncover its function, *MDFI* was both knocked down and overexpressed in NSCLC cells. We found that MDFI promotes malignant behaviors in NSCLC cells, aligning with its previously reported tumor-enhancing role in GC and CRC [16–18]. These findings suggest that MDFI may serve as an oncogene in NSCLC progression and could represent a potential therapeutic target.

Autophagy is a cellular self-degradation process that plays a critical role in maintaining intracellular homeostasis [32]. Dysfunction of autophagy has been associated with the pathogenesis of various clinical conditions, including cancer, cardiovascular diseases, respiratory problems, and neurodegenerative disorders [33]. The LC3-II/I ratio is a widely recognized marker that can directly reflect autophagic activity [34]. Conversely, the accumulation of p62 protein is negatively correlated with autophagy activity; its levels decrease when autophagy is increased [35]. Furthermore, ATG12, a critical regulator in the autophagy pathway, is crucial for autophagosome formation and overall autophagic modulation [36]. Through bioinformatic analysis using the HitPredict database, we observed a potential interaction between MDFI and ATG12. Furthermore, to explore whether MDFI expression impacts NSCLC progression through autophagy, the expression levels of p62 and ATG12, along with the LC3II/I ratio, were assessed. Analysis revealed that *MDFI* knockdown decreased the LC3II/I ratio and reduced the expression levels of ATG12, alongside increasing the p62 expression. In contrast, *MDFI* overexpression showed an opposite trend. Interestingly, treatment with 3-MA reversed the effects of *MDFI* overexpression on malignant behavior and autophagy marker proteins in NSCLC cells. Additionally, to validate these observations *in vivo*, tumor formation experiments were performed in nude mice. Ki-67, a well-known marker of cell proliferation, has been associated with tumor growth, recurrence, and metastasis [37–39]. In our study, tumor volume, tumor weight, and Ki-67 expression levels were substantially reduced in the *MDFI* knockdown group, suggesting inhibition of tumor growth. Consistent with *in vitro* results, tumors from the *MDFI* knockdown group showed decreased LC3II/I ratio and ATG12 expression, along with increased p62 levels. Overall, these findings support the oncogenic role of MDFI in NSCLC progression, possibly mediated by its effect on autophagy.

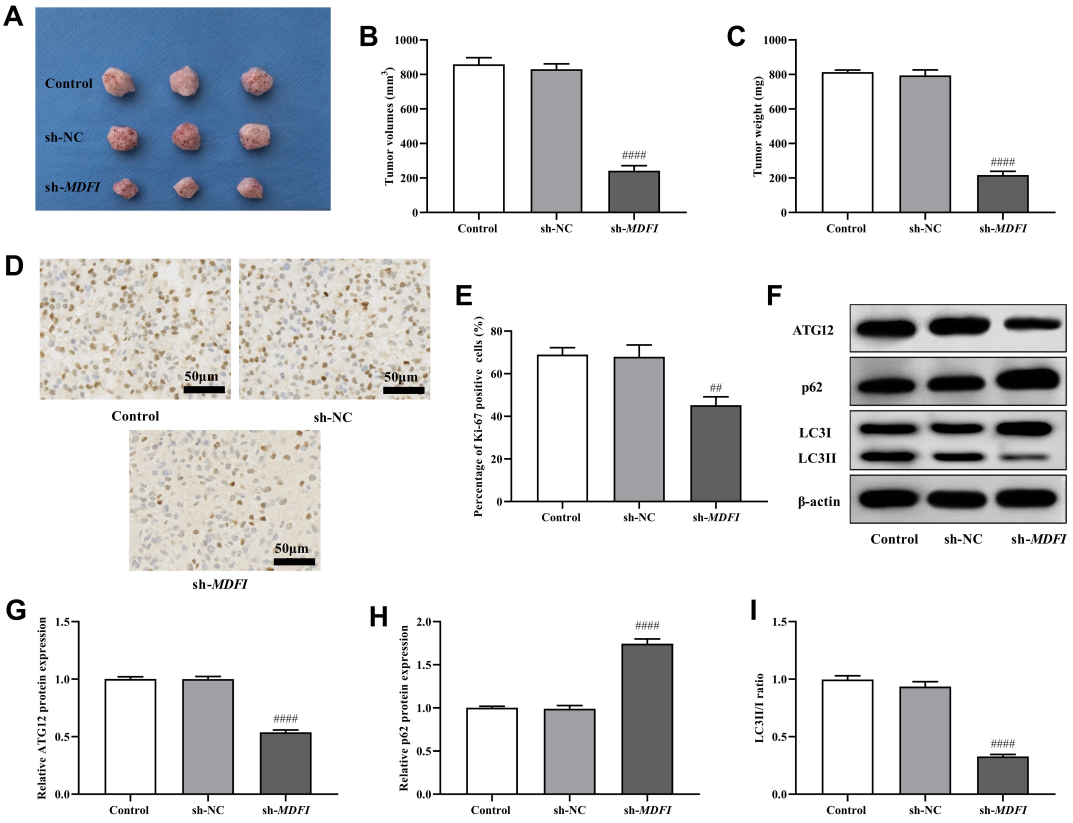

Fig. 10. Impact of MDFI on tumor formation *in vivo*. (A) Anatomical gross images of tumor tissue from the nude mouse tumorigenesis experiment (n = 3). (B,C) Statistical analysis of tumor volume and weight in each group (n = 3). (D,E) The expression levels of Ki-67 protein were assessed using immunohistochemistry (scale bar: 50 μm, magnification: 20×) (n = 3). (F) Expression levels of ATG12, p62, and LC3II/I (Western blot analysis, n = 3). (G–I) Graphical presentation of ATG12 and p62 expression, and LC3II/I ratio (n = 3). $^{\#\#}p < 0.01$, $^{\#\#\#\#}p < 0.0001$, compared to the sh-NC group. Ki-67, nuclear proliferation-associated antigen.

This study assessed the regulatory role of MDFI in NSCLC and found that MDFI promotes malignant behavior in NSCLC cells, likely through the regulation of autophagy. However, this study also has certain limitations. Due to limited funding and the unavailability of experimental resources and patient samples, this study was confined to *in vitro* cellular models and *in vivo* nude mouse models. Further investigation involving patient samples is needed to validate the role of MDFI in NSCLC and explain its potential mechanisms. Although the impact of MDFI on NSCLC cell proliferation, migration, invasion, and autophagy was confirmed, the specific molecular mechanisms by which MDFI regulates autophagy are yet to be fully explored. Our bioinformatic analysis using the HitPredict database demonstrated potential interaction between MDFI and ATG12; however, our study did not experimentally confirm the nature of this interaction in the context of autophagy modulation. Previous studies have shown that ATG12 is regulated by various factors during cancer-associated autophagy, such as miRNAs, the Wiskott-Aldrich protein family, the epidermal growth factor receptor, and circular RNAs [40–44]. Moreover, studies have found that MDFI regulates cancer progression through the AKT and the Wnt/β-catenin signaling pathway [17,18], which are known to play a crucial role in autophagy regulation [45–47]. Based on these observations, we infer that MDFI may impact autophagy in NSCLC through intermediates, such as ATG12 or AKT, and the Wnt/β-catenin signal pathway. Future studies with improved experimental conditions should experimentally validate these assumptions and elucidate the precise molecular mechanisms of MDFI underlying NSCLC. Furthermore, with access to a larger cohort of clinical specimens, the diagnostic and prognostic significance of MDFI expression in NSCLC patients would be further explored.

Conclusion

In summary, this study reveals that the upregulation of MDFI enhances autophagy and promotes the malignant progression of NSCLC cells. The findings offer a comprehensive understanding of NSCLC pathogenesis and underscore MDFI as a potential biomarker and therapeutic target.

Availability of Data and Materials

The data used to support the findings of this study are available from the corresponding author upon request.

Author Contributions

GLM and YGR designed the research study. GLM, JL, MLY, and YGR performed the research. GLM, JL, and MLY collected and analyzed the data. All authors have been involved in drafting the manuscript and critically revising it. All authors have participated sufficiently in the work to take public responsibility for appropriate portions of the content and agreed to be accountable for all aspects of the work in ensuring that questions related to its accuracy or integrity are addressed. All authors read and approved the final manuscript.

Ethics Approval and Consent to Participate

All experiments were performed following the relevant ethical guidelines and regulations. Experimental protocols involving animals were approved by the Ethics Committee of Jinan People's Hospital Affiliated to Shandong First Medical University (Ethical approval number: 2025-lw-26) and adhered to Animal Research: Reporting of *In Vivo* Experiments (ARRIVE) guidelines for the reporting of animal experiments.

Acknowledgment

Not applicable.

Funding

This research received no external funding.

Conflict of Interest

The authors declare no conflict of interest.

Supplementary Material

Supplementary material associated with this article can be found in the online version, at https://doi.org/10.24976/Discov.Med.202537199.145.

References

[1] Stravopodis DJ, Papavassiliou KA, Papavassiliou AG. Vistas in Non-Small Cell Lung Cancer (NSCLC) Treatment: of Kinome and Signaling Networks. International Journal of Biological Sciences. 2023; 19: 2002–2005. https://doi.org/10.7150/ijbs.83574.

[2] Duma N, Santana-Davila R, Molina JR. Non-Small Cell Lung Cancer: Epidemiology, Screening, Diagnosis, and Treatment. Mayo Clinic Proceedings. 2019; 94: 1623–1640. https://doi.org/10.1016/j.mayocp.2019.01.013.

[3] Alduais Y, Zhang H, Fan F, Chen J, Chen B. Non-small cell lung cancer (NSCLC): A review of risk factors, diagnosis, and treatment. Medicine. 2023; 102: e32899. https://doi.org/10.1097/MD.0000000000032899.

[4] Zhao Y, Guo S, Deng J, Shen J, Du F, Wu X, *et al*. VEGF/VEGFR-Targeted Therapy and Immunotherapy in Non-small Cell Lung Cancer: Targeting the Tumor Microenvironment. International Journal of Biological Sciences. 2022; 18: 3845–3858. https://doi.org/10.7150/ijbs.70958.

[5] Wang J, Gong M, Fan X, Huang D, Zhang J, Huang C. Autophagy-related signaling pathways in non-small cell lung cancer. Molecular and Cellular Biochemistry. 2022; 477: 385–393. https://doi.org/10.1007/s11010-021-04280-5.

[6] Tao Z, Liu L, Zheng LD, Cheng Z. Autophagy in Adipocyte Differentiation. Methods in Molecular Biology (Clifton, N.J.). 2019; 1854: 45–53. https://doi.org/10.1007/7651_2017_65.

[7] Li X, He S, Ma B. Autophagy and autophagy-related proteins in cancer. Molecular Cancer. 2020; 19: 12. https://doi.org/10.1186/s12943-020-1138-4.

[8] Yang Y, Klionsky DJ. Autophagy and disease: unanswered questions. Cell Death and Differentiation. 2020; 27: 858–871. https://doi.org/10.1038/s41418-019-0480-9.

[9] Zhang J, Xiang Q, Wu M, Lao YZ, Xian YF, Xu HX, *et al*. Autophagy Regulators in Cancer. International Journal of Molecular Sciences. 2023; 24: 10944. https://doi.org/10.3390/ijms241310944.

[10] Liang J, Zhang L, Cheng W. Non-coding RNA-mediated autophagy in cancer: A protumor or antitumor factor? Biochimica et Biophysica Acta. Reviews on Cancer. 2021; 1876: 188642. https://doi.org/10.1016/j.bbcan.2021.188642.

[11] Hu X, Wen L, Li X, Zhu C. Relationship Between Autophagy and Drug Resistance in Tumors. Mini Reviews in Medicinal Chemistry. 2023; 23: 1072–1078. https://doi.org/10.2174/1389557522666220905090732.

[12] Guo W, Du K, Luo S, Hu D. Recent Advances of Autophagy in Non-Small Cell Lung Cancer: From Basic Mechanisms to Clinical Application. Frontiers in Oncology. 2022; 12: 861959. https://doi.org/10.3389/fonc.2022.861959.

[13] Houser JS, Patel M, Wright K, Onopiuk M, Tsiokas L, Humphrey MB. The inhibitor of MyoD Family A (I-MFA) regulates megakaryocyte lineage commitment and terminal differentiation. Blood Cells, Molecules & Diseases. 2023; 102: 102760. https://doi.org/10.1016/j.bcmd.2023.102760.

[14] Shotorbani PY, Chaudhari S, Tao Y, Tsiokas L, Ma R. Inhibitor of myogenic differentiation family isoform a, a new positive regulator of fibronectin production by glomerular mesangial cells. American Journal of Physiology. Renal Physiology. 2020; 318: F673–F682. https://doi.org/10.1152/ajprenal.00508.2019.

[15] Lu T, Zhu Y, Guo J, Mo Z, Zhou Q, Hu CY, *et al*. MDFI regulates fast-to-slow muscle fiber type transformation via the calcium signaling pathway. Biochemical and Biophysical Research Communications. 2023; 671: 215–224. https://doi.org/10.1016/j.bbrc.2023.05.053.

[16] Sui Y, Li X, Oh S, Zhang B, Freeman WM, Shin S, *et al*. Opposite Roles of the JMJD1A Interaction Partners MDFI and MDFIC in Colorectal Cancer. Scientific Reports. 2020; 10: 8710. https://doi.org/10.1038/s41598-020-65536-6.

[17] Ma D, Liu S, Liu K, Kong L, Xiao L, Xin Q, *et al*. MDFI promotes the proliferation and tolerance to chemotherapy of colorectal cancer cells by binding ITGB4/LAMB3 to activate the AKT signaling pathway. Cancer Biology & Therapy. 2024; 25: 2314324. https://doi.org/10.1080/15384047.2024.2314324.

[18] Mi C, Zhao Y, Ren L, Zhang D. Inhibition of MDFI attenuates proliferation and glycolysis of Helicobacter pylori-infected gastric cancer cells by inhibiting Wnt/β-catenin pathway. Cell Biology International. 2022; 46: 2198–2206. https://doi.org/10.1002/cbin.11907.

[19] Chen P, Quan Z, Song X, Gao Z, Yuan K. *MDFI* is a novel biomarker for poor prognosis in LUAD. Frontiers in Oncology. 2022; 12: 1005962. https://doi.org/10.3389/fonc.2022.1005962.

[20] Ning F, Wang H, Liang Z, Lan J. *TNFAIP3* Overexpression Inhibits Diffuse Large B-Cell Lymphoma Progression by Promoting Autophagy through TLR4/MyD88/NF-κB Signaling Pathway. Discovery Medicine. 2024; 36: 1627–1640. https://doi.org/10.24976/Discov.Med.202436187.149.

[21] Shen J, Meng Y, Wang K, Gao M, Du J, Wang J, *et al*. EML4-ALK G1202R mutation induces EMT and confers resistance to ceritinib in NSCLC cells via activation of STAT3/Slug signaling. Cellular Signalling. 2022; 92: 110264. https://doi.org/10.1016/j.cellsig.2022.110264.

[22] Meng Q, Li Y, Sun Z, Liu J. Citrulline facilitates the glycolysis, proliferation, and metastasis of lung cancer cells by regulating RAB3C. Environmental Toxicology. 2024; 39: 4372–4384. https://doi.org/10.1002/tox.24326.

[23] Jiang M, Bai H, Fang S, Zhou C, Shen W, Gong Z. CircLIFRSA/miR-1305/PTEN axis attenuates malignant cellular processes in non-small cell lung cancer by regulating AKT phosphorylation. Molecular Cancer. 2024; 23: 208. https://doi.org/10.1186/s12943-024-02120-w.

[24] Zhao H, Wang Y, He Y, Zhang P, Zeng C, Du T, *et al*. ANKRD29, as a new prognostic and immunological biomarker of non-small cell lung cancer, inhibits cell growth and migration by regulating MAPK signaling pathway. Biology Direct. 2023; 18: 28. https://doi.org/10.1186/s13062-023-00385-7.

[25] Ho HL, Lin SC, Chiang CW, Lin C, Liu CW, Yeh YC, *et al*. miR-193b-3p suppresses lung cancer cell migration and invasion through PRNP targeting. Journal of Biomedical Science. 2025; 32: 28. https://doi.org/10.1186/s12929-025-01121-1.

[26] Fan M, Liu Q, Ma X, Jiang Y, Wang Y, Jia S, *et al*. ZNF131-BACH1 transcriptionally accelerates RAD51-dependent homologous recombination repair and therapy-resistance of non-small-lung cancer cells by preventing their degradation from CUL3. Theranostics. 2024; 14: 7241–7264. https://doi.org/10.7150/thno.97593.

[27] Zhao G, Feng E, Liu Y. Efficacy and safety of veliparib combined with traditional chemotherapy for treating patients with lung cancer: a comprehensive review and meta-analysis. PeerJ. 2023; 11: e16402. https://doi.org/10.7717/peerj.16402.

[28] Pallis AG, Syrigos KN. Lung cancer in never smokers: disease characteristics and risk factors. Critical Reviews in Oncology/hematology. 2013; 88: 494–503. https://doi.org/10.1016/j.critrevonc.2013.06.011.

[29] Xia J, Zhang J, Xiong Y, Zhao J, Zhou Y, Jiang T, *et al*. Circulating tumor DNA minimal residual disease in clinical practice of non-small cell lung cancer. Expert Review of Molecular Diagnostics. 2023; 23: 913–924. https://doi.org/10.1080/14737159.2023.2252334.

[30] Thébault S, Mesnard JM. How the sequestration of a protein interferes with its mechanism of action: example of a new family of proteins characterized by a particular cysteine-rich carboxy-terminal domain involved in gene expression regulation. Current Protein & Peptide Science. 2001; 2: 155–167. https://doi.org/10.2174/1389203013381143.

[31] Vafaeie F, Nomiri S, Ranjbaran J, Safarpour H. ACAN, MDFI, and CHST1 as Candidate Genes in Gastric Cancer: A Comprehensive Insilco Analysis. Asian Pacific Journal of Cancer Prevention: APJCP. 2022; 23: 683–694. https://doi.org/10.31557/APJCP.2022.23.2.683.

[32] Guhe V, Soni B, Ingale P, Singh S. Autophagy proteins and its homeostasis in cellular environment. Advances in Protein Chemistry and Structural Biology. 2021; 123: 73–93. https://doi.org/10.1016/bs.apcsb.2019.12.002.

[33] Klionsky DJ, Petroni G, Amaravadi RK, Baehrecke EH, Ballabio A, Boya P, *et al*. Autophagy in major human diseases. The EMBO Journal. 2021; 40: e108863. https://doi.org/10.15252/embj.2021108863.

[34] Zeng Z, Liang J, Wu L, Zhang H, Lv J, Chen N. Exercise-Induced Autophagy Suppresses Sarcopenia Through Akt/mTOR and Akt/FoxO3a Signal Pathways and AMPK-Mediated Mitochondrial Quality Control. Frontiers in Physiology. 2020; 11: 583478. https://doi.org/10.3389/fphys.2020.583478.

[35] Bjørkøy G, Lamark T, Pankiv S, Øvervatn A, Brech A, Johansen T. Monitoring autophagic degradation of p62/SQSTM1. Methods in Enzymology. 2009; 452: 181–197. https://doi.org/10.1016/S0076-6879(08)03612-4.

[36] Mizushima N. The ATG conjugation systems in autophagy. Current Opinion in Cell Biology. 2020; 63: 1–10. https://doi.org/10.1016/j.ceb.2019.12.001.

[37] Andrés-Sánchez N, Fisher D, Krasinska L. Physiological functions and roles in cancer of the proliferation marker Ki-67. Journal of Cell Science. 2022; 135: jcs258932. https://doi.org/10.1242/jcs.258932.

[38] Luo Z, Yan X, Liu Y, Nan F, Lei Y, Ren Y, *et al*. Prognostic significance of Ki-67 in assessing the risk of progression, relapse or metastasis in pheochromocytomas and paragangliomas. Annals of Medicine. 2025; 57: 2478312. https://doi.org/10.1080/07853890.2025.2478312.

[39] Tian J, Chen W. Prediction of Ki-67 expression and malignant potential in gastrointestinal stromal tumors: novel models based on CE-CT and serological indicators. BMC Cancer. 2024; 24: 1412. https://doi.org/10.1186/s12885-024-13172-y.

[40] Song H, Zhao Z, Ma L, Zhang B, Song Y. MiR-3653 blocks autophagy to inhibit epithelial-mesenchymal transition in breast cancer cells by targeting the autophagy-regulatory genes ATG12 and AMBRA1. Chinese Medical Journal. 2023; 136: 2086–2100. https://doi.org/10.1097/CM9.0000000000002569.

[41] Hu JL, He GY, Lan XL, Zeng ZC, Guan J, Ding Y, *et al*. Inhibition of ATG12-mediated autophagy by miR-214 enhances radiosensitivity in colorectal cancer. Oncogenesis. 2018; 7: 16. https://doi.org/10.1038/s41389-018-0028-8.

[42] Nie Y, Liang X, Liu S, Guo F, Fang N, Zhou F. WASF3 Knockdown Sensitizes Gastric Cancer Cells to Oxaliplatin by Inhibiting ATG12-Mediated Autophagy. The American Journal of the Medical Sciences. 2020; 359: 287–295. https://doi.org/10.1016/j.amjms.2020.02.007.

[43] Chen Y, Wang R, Huang S, Henson ES, Bi J, Gibson SB. Erbb2 Receptor Tyrosine Kinase 2 (ERBB2) Promotes ATG12-Dependent Autophagy Contributing to Treatment Resistance of Breast Cancer Cells. Cancers. 2021; 13: 1038. https://doi.org/10.3390/cancers13051038.

[44] Luo M, Deng X, Chen Z, Hu Y. Circular RNA circPOFUT1 enhances malignant phenotypes and autophagy-associated chemoresistance via sequestrating miR-488-3p to activate the PLAG1-ATG12 axis in gastric cancer. Cell Death & Disease. 2023; 14: 10. https://doi.org/10.1038/s41419-022-05506-0.

[45] Noguchi M, Hirata N, Suizu F. The links between AKT and two intracellular proteolytic cascades: ubiquitination and autophagy. Biochimica et Biophysica Acta. 2014; 1846: 342–352. https://doi.org/10.1016/j.bbcan.2014.07.013.

[46] Lorzadeh S, Kohan L, Ghavami S, Azarpira N. Autophagy and the Wnt signaling pathway: A focus on Wnt/β-catenin signaling. Biochimica et Biophysica Acta. Molecular Cell Research. 2021; 1868: 118926. https://doi.org/10.1016/j.bbamcr.2020.118926.

[47] Ma Q, Yu J, Zhang X, Wu X, Deng G. Wnt/β-catenin signaling pathway-a versatile player in apoptosis and autophagy. Biochimie. 2023; 211: 57–67. https://doi.org/10.1016/j.biochi.2023.03.001.